The Abdus Salam International Centre for Theoretical Physics

United Nations Educational, Scientific and Cultural Organization

IAEA
International Atomic Energy Agency

1953-42

**International Workshop on the Frontiers of Modern Plasma Physics**

***14 - 25 July 2008***

# Global modes in spatially limited plasmas.

J. Vranjes

*K.U. Leuven, Centre for Plasma Astrophysics*
*Belgium*

# Global modes in spatially limited plasmas

J. Vranjes

Centrum voor Plasma-Astrofysica
Katholieke Universiteit Leuven
http://wis.kuleuven.be/cpa

AS ICTP, Trieste, July 2008

- Topics studied:
  - electron plasma
  - drift modes (electrostatic, electromagnetic, streaming/rotating plasma, dusty plasma, experimental argon plasma)
  - pair plasma (electron-positron, pair-ion)
- Coworkers:
  - M. Y. Tanaka (+ team members)
  - H. Saleem (+ team members)
  - S. Poedts
  - M. Kono
  - P. K. Shukla

# Global and local

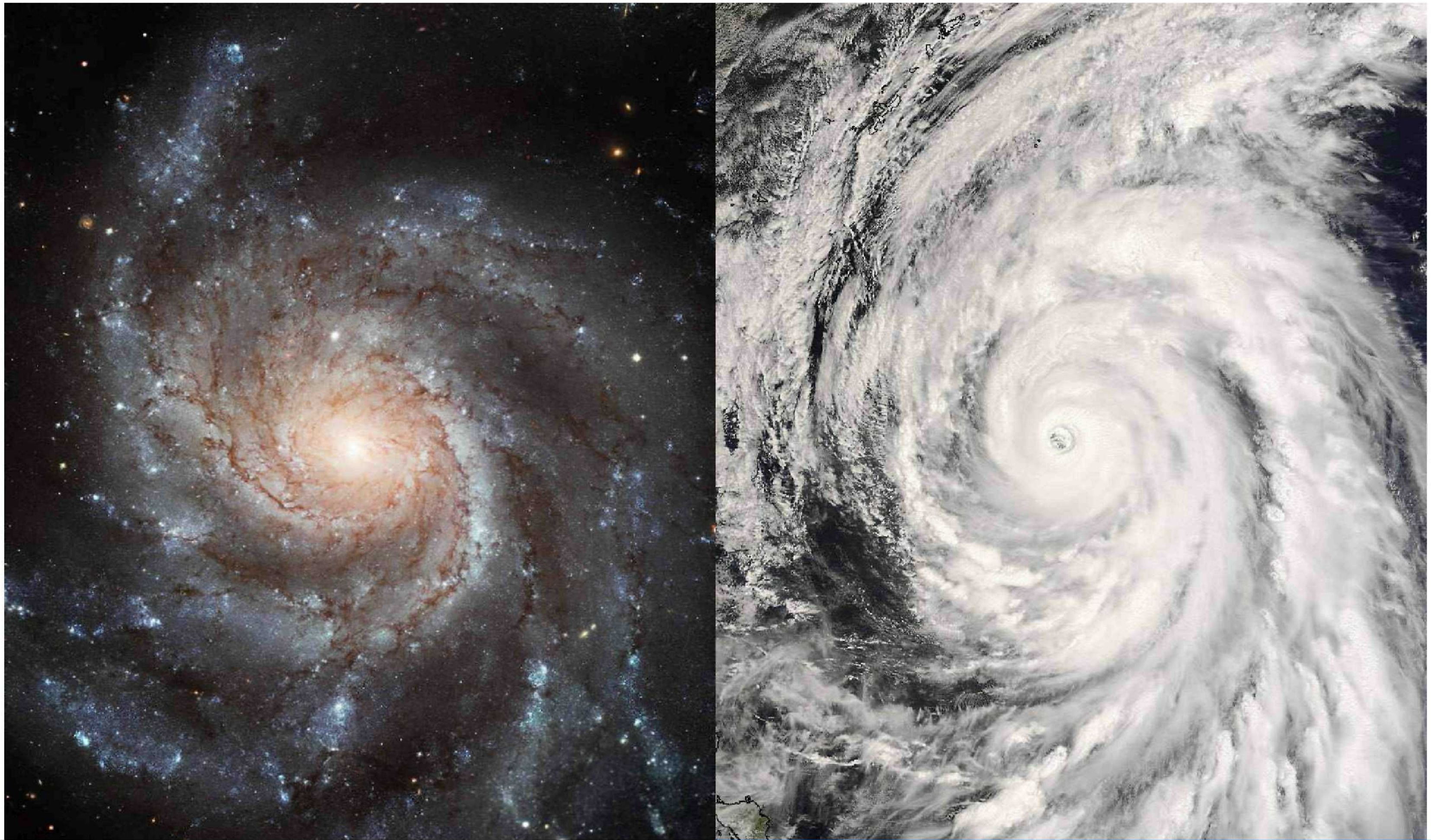

# Outline

# Outline

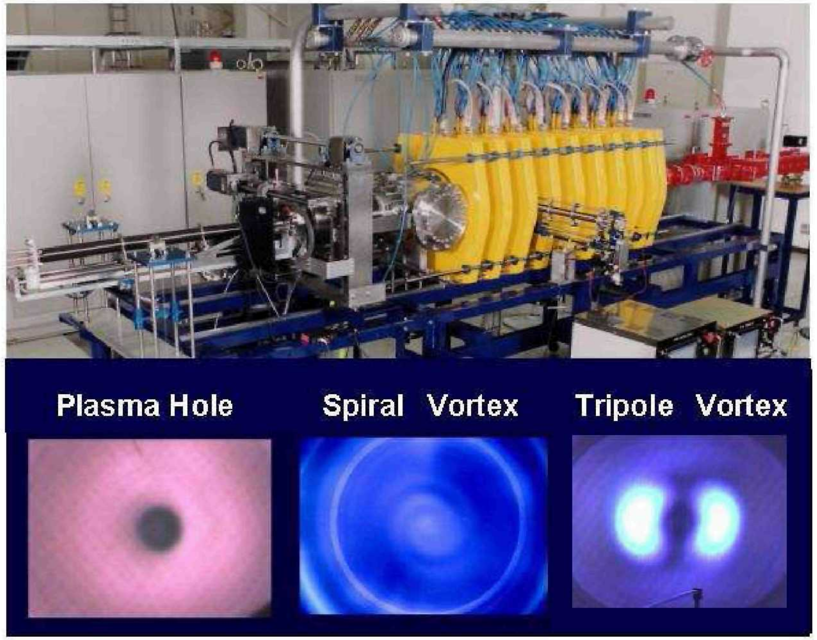


- *Kono and Tanaka PRL (2000)*
- *Vranjes et al. PRL (2002)*
- *Nagaoka et al. PRL (2002)*

# A global spiral vortex

- Vranjes et al., Phys. Rev. Lett. **89**, 265002 (2002)

$$\left[\frac{\partial}{\partial t}+\frac{1}{B_0}\vec{e}_z\times\nabla_\perp(\Phi_1+B_0\varphi)\cdot\nabla_\perp\right]\left[(1-\rho^2\nabla_\perp^2)\right.$$
$$\left.\times(\Phi_1+B_0\varphi)-B_0(\varphi+\psi)\right]+\frac{T_e}{e}\nabla_\parallel\cdot\vec{v}_\parallel=0. \quad (1)$$

$$[\partial/\partial t+\vec{e}_z\times\nabla_\perp(\Phi_1+B_0\varphi)\cdot\nabla_\perp/B_0]\,v_\parallel=0.$$

$$\Phi_1=\phi_1+\phi_{n1}\approx[\phi_1+(T_n/e)\log n_{n1}]\Omega_i^2/(\Omega_i^2+\nu_i^2).$$

$$\vec{v}_{i0}\equiv\vec{e}_\theta d\varphi(r)/dr=\vec{e}_\theta(d\Phi_0/dr)/B_0-[1/(r\Omega_{ef}B_0^2)](d\Phi_0/dr)^2\vec{e}_\theta,$$

$$\rho=c_s/\Omega_{ef},\quad \Omega_{ef}\equiv\Omega_i/[\Omega_i^2/(\Omega_i^2+\nu_i^2)],\quad v_*\equiv d\psi(r)/dr=-n_0'c_s^2/n_0\Omega_{ef}.$$

- Vranjes et al., Phys. Rev. Lett. **89**, 265002 (2002)

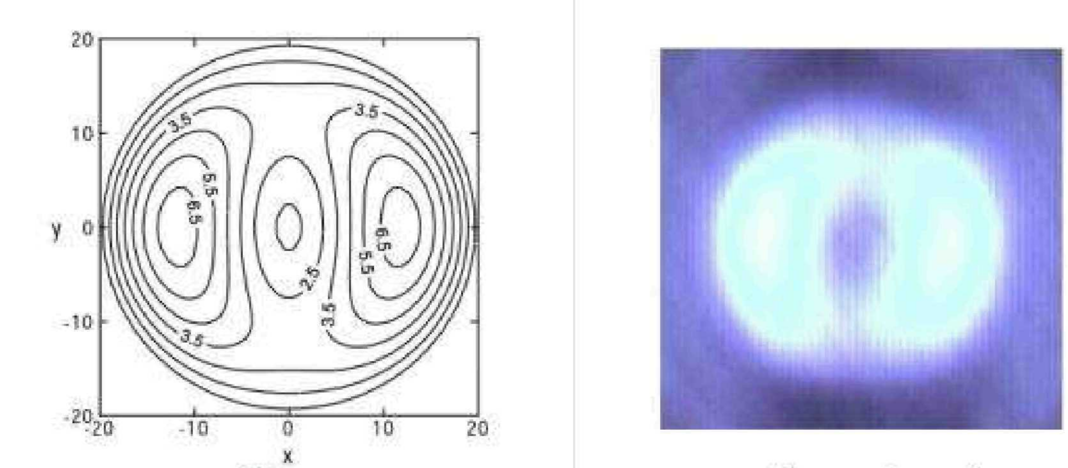


Theory

Experiments

# Vortices in simple torus

- The structures observed in helium plasmas evolving in time and rotating in the poloidal cross-section with a period of about $100\mu$s.
- Monopolar vortices + dipolar vortices.
- Dipole: two components rotate around their centers in opposite directions. The whole structure rotates in poloidal direction.
- Generated mainly in the region where the magnetic field curvature is opposite to the density gradient, that is in most of the region outside the centre of the cross-section.

- Large bursty flux events occur at the vortex separatrices whenever a double vortex in the potential is formed.

- When they occur, they cover most of the plasma cross-section.

# Blaamann torus

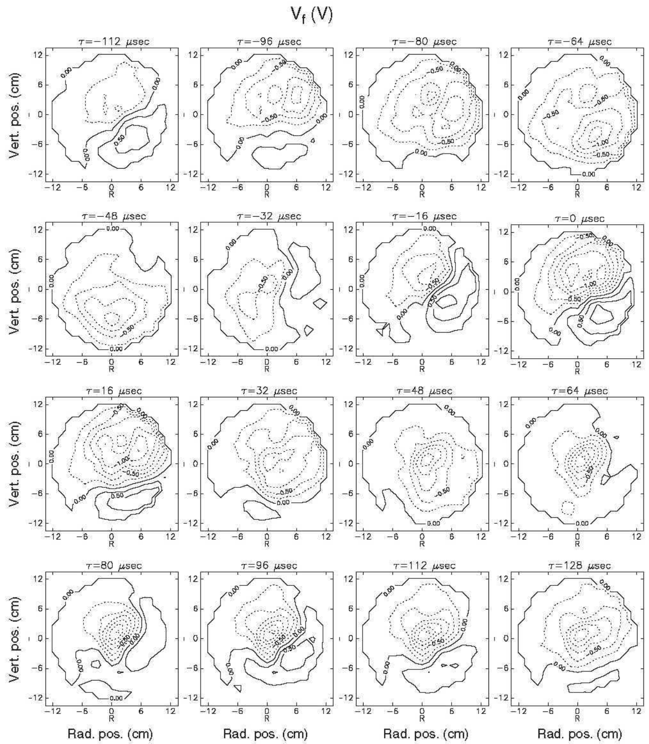

**Figure 3.** Two-dimensional contour plots of floating potential fluctuations derived by conditional averaging. The temporal evolution starts at $-112\,\mu s$ with respect to the reference signal event and is plotted every 16 up to $128\,\mu s$. Radial positions and vertical positions are given in centimetres from the centre of cross-section.

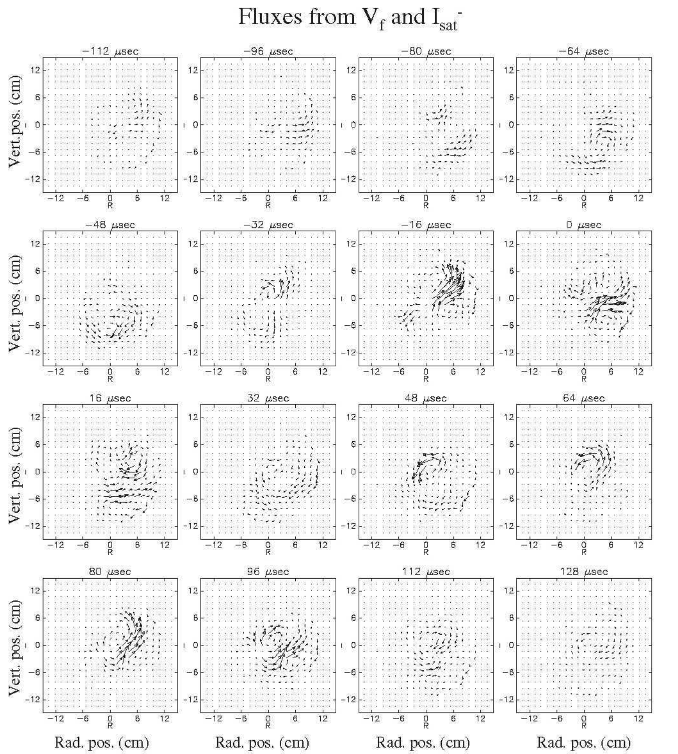

**Figure 5.** Two-dimensional contour plots of particle fluxes. The temporal evolution starts at $-112\,\mu s$ with respect to the reference signal event and is plotted every 16 up to $128\,\mu s$. Radial positions and vertical positions are given in centimetres from the centre of cross-section.

Fredriksen et al. *Plasma Phys. Control. Fusion* **45**, *721 (2003)*

# Stellarator

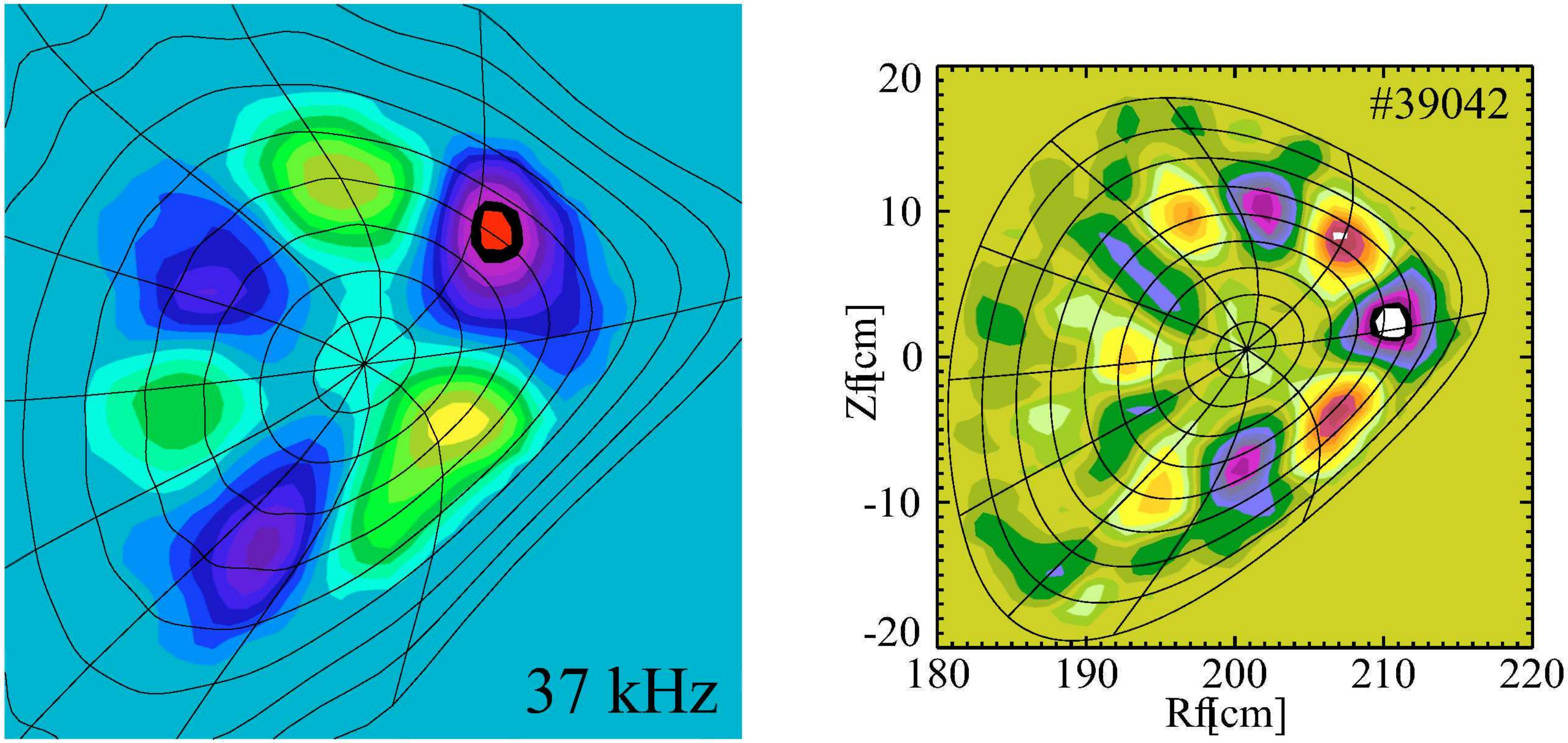

# Linear machine

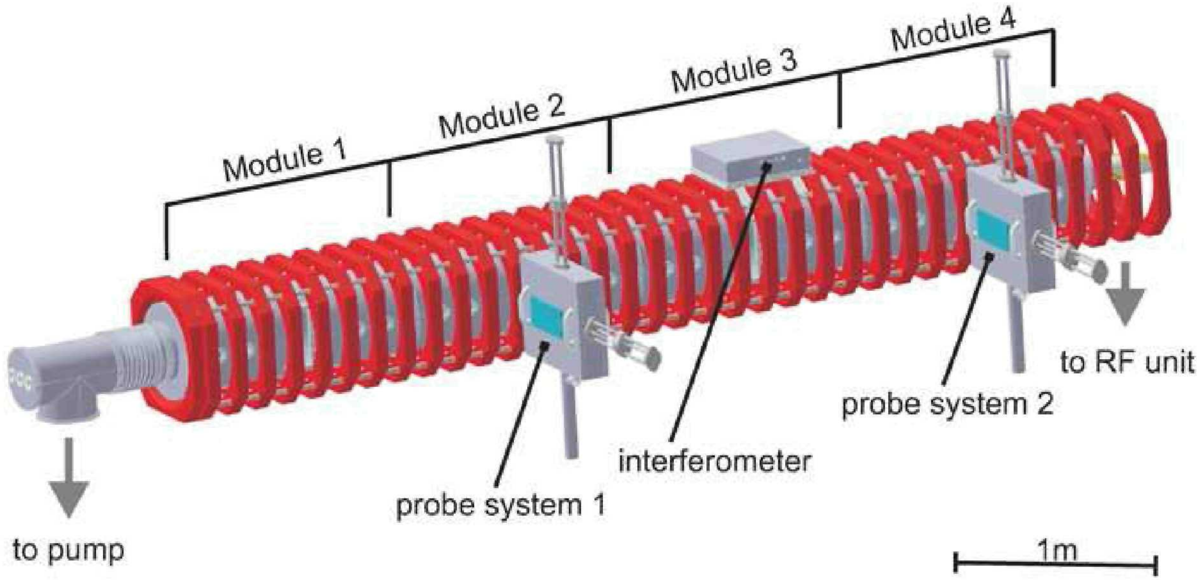


**Figure 1.** Schematic of the VINETA device, including the azimuthal probe positing systems.

*Grulke* et al., *PPCF* **49**, *B247 (2007)*

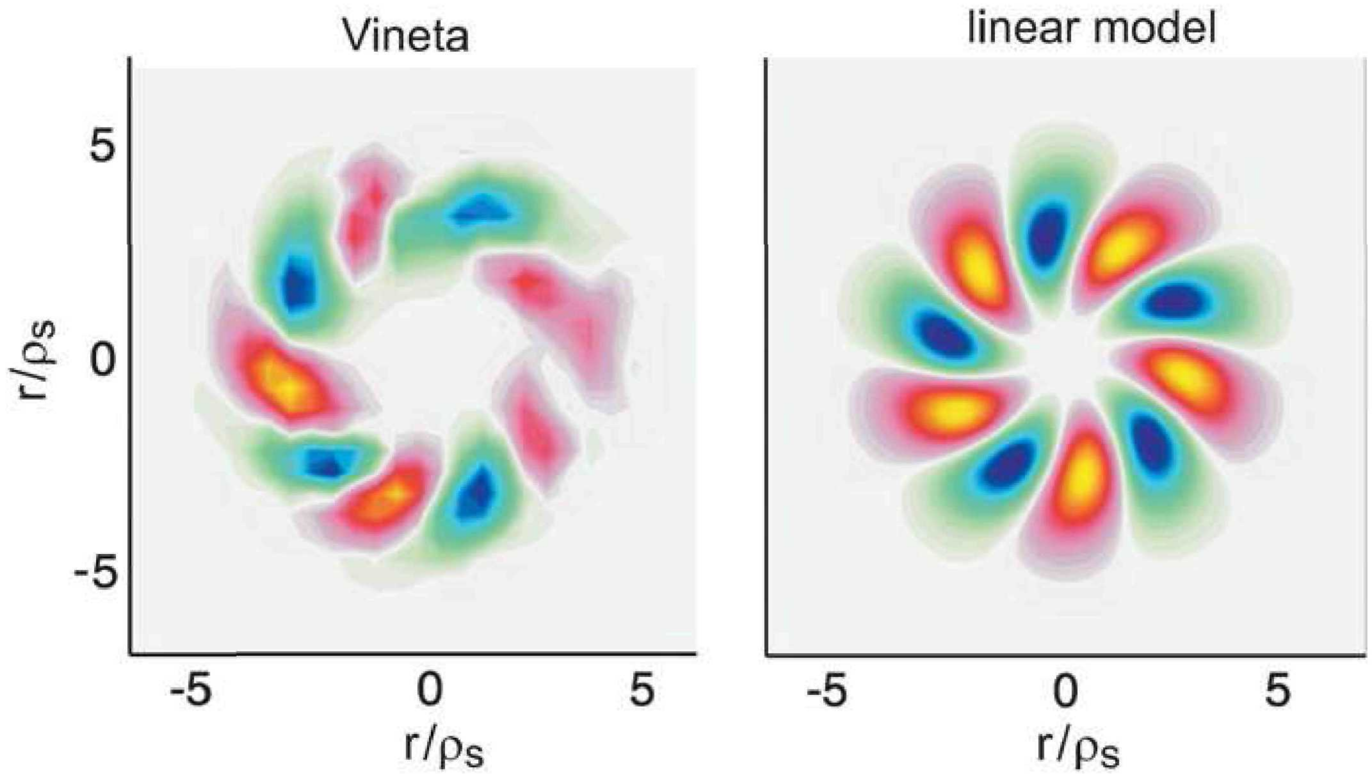


*Grulke* et al., *PPCF* **49**, *B247 (2007)*

# Pure electron plasma

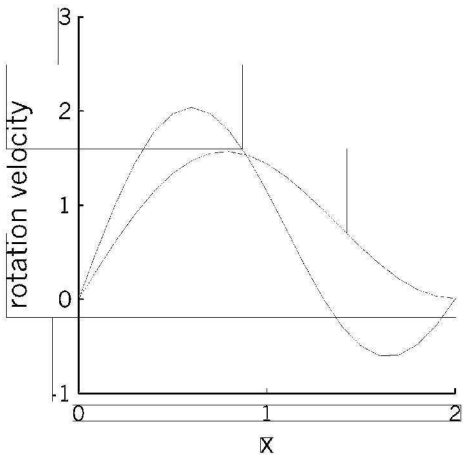


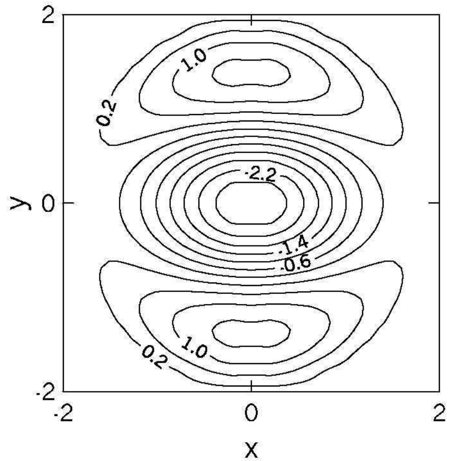


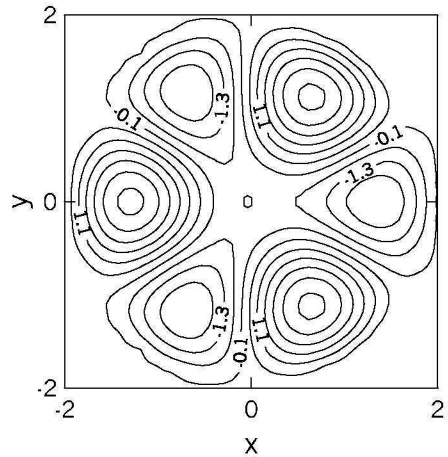


*J. Vranjes, P.K. Shukla, M. Kono, and S. Poedts, PoP* **8**, *3165-3176 (2001)*

## Outline

# Space plasma

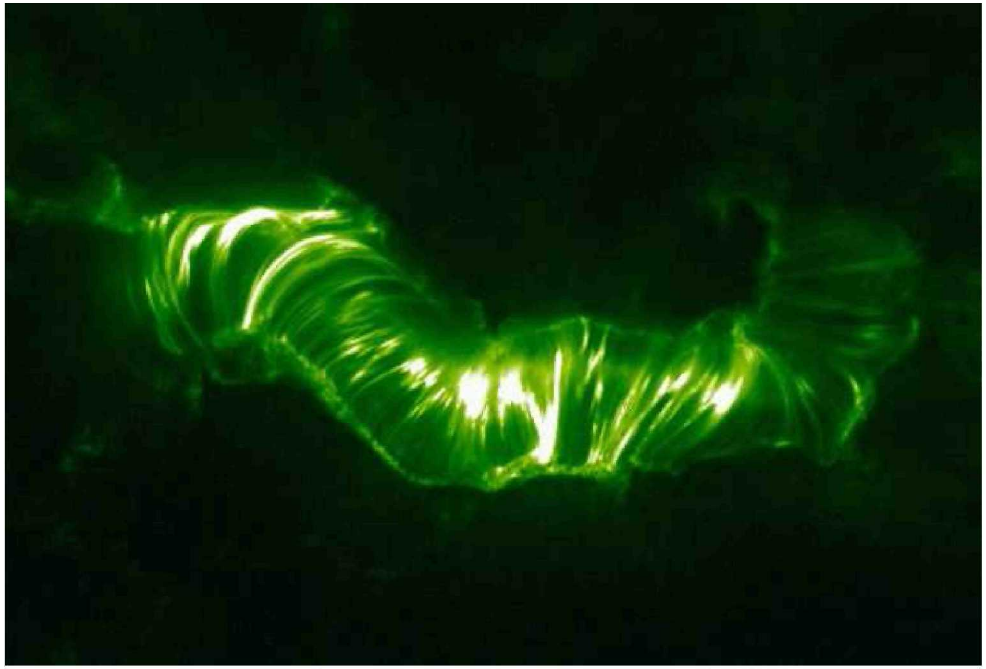

*Solar arcade*

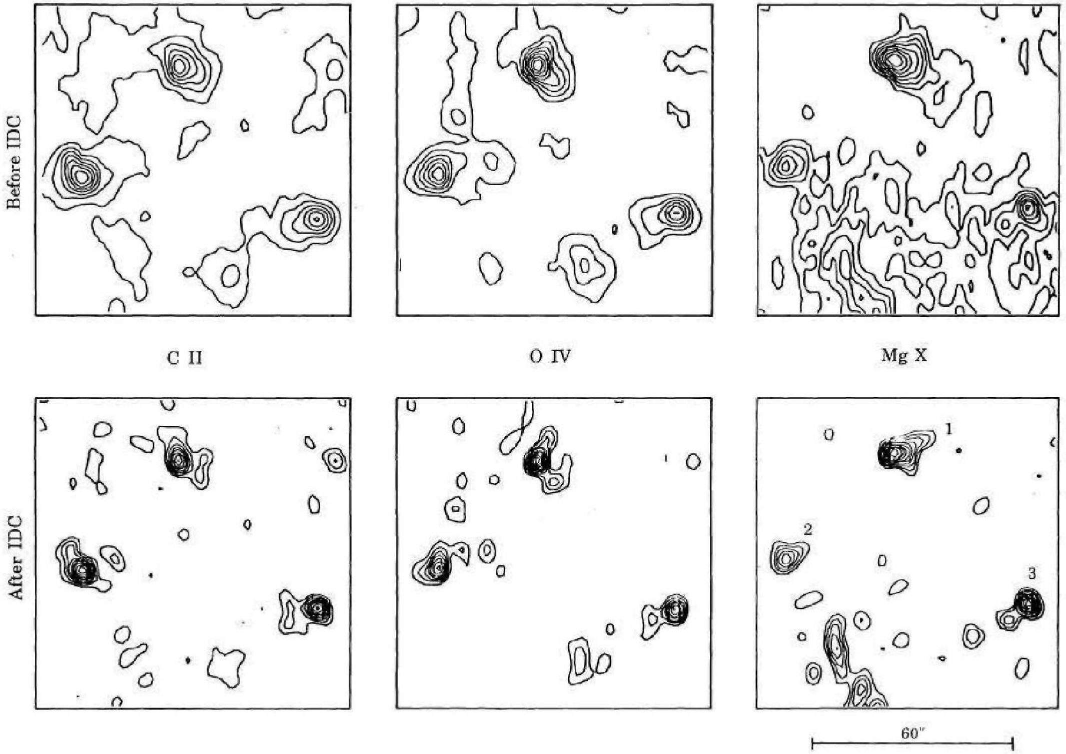


*Karovska and Habal, ApJ* **371**, *402 (1991)*

# Carina nebula

# Some discrete clouds

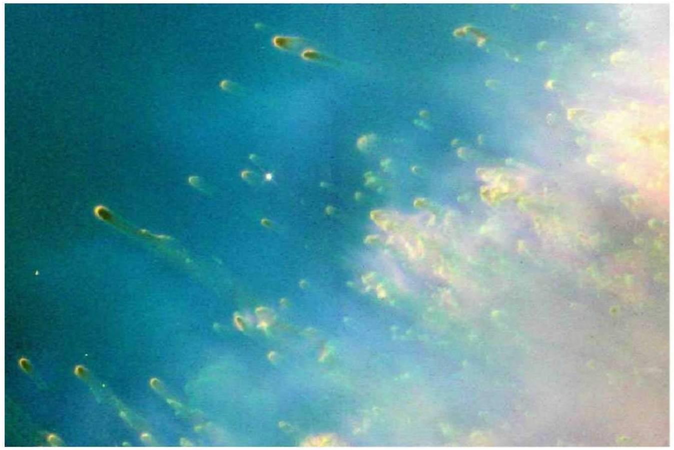

# Filaments

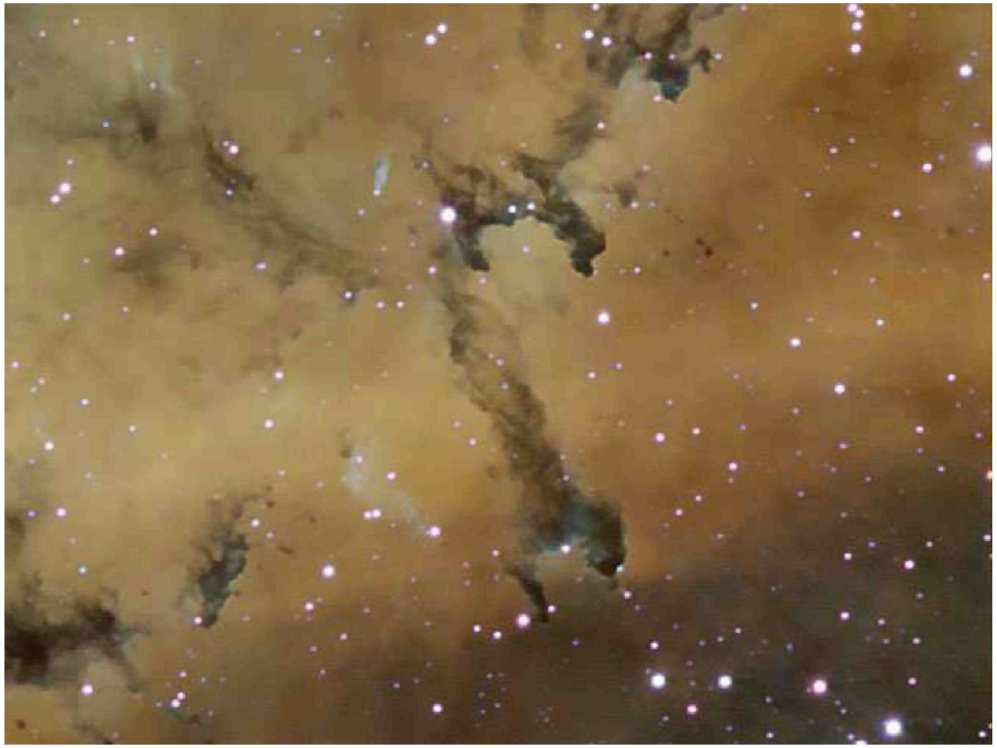

*Rosette nebula: twisted mode with poloidal number* $m = 3$.

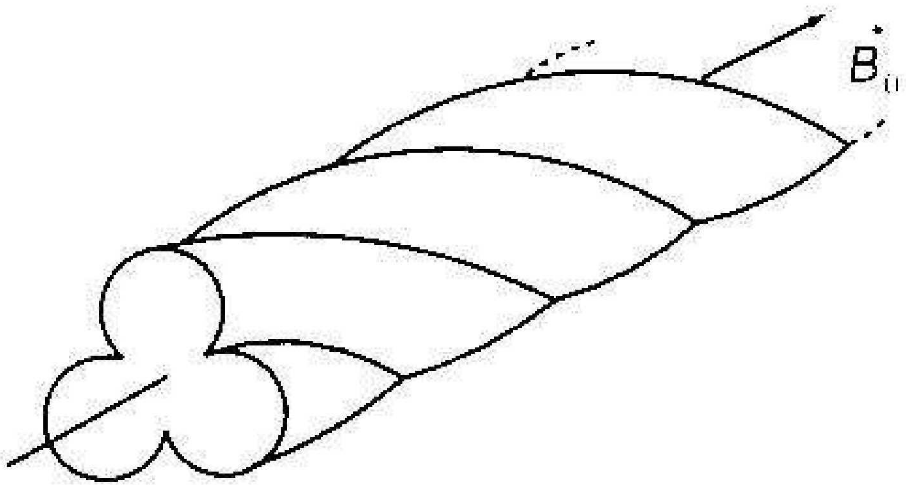
$B_0$

## Rosette nebula

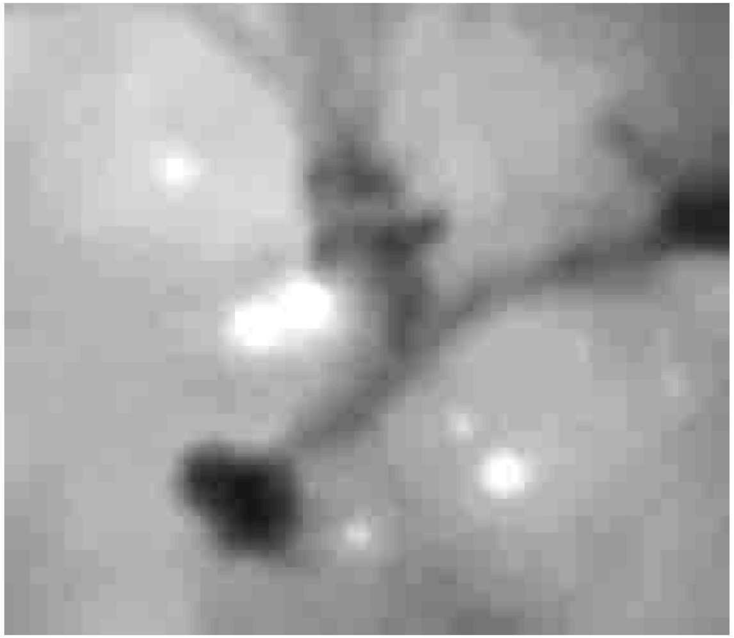

*P. Carlqvist et al. Astron. Astrophys.* **403**, *399 (2003)*

# Coupled potentials

$$\nabla_\perp^2 \frac{\partial^2 \phi_1}{\partial t^2} - \frac{B_0}{\Omega_d} \nabla_\perp^2 \frac{\partial^2 \varphi_1}{\partial t^2} - \left(\frac{\partial^2}{\partial t^2} + \Omega_d^2\right)\left(\frac{1}{c_d^2}\frac{\partial^2}{\partial t^2} - \frac{\partial^2}{\partial z^2}\right)\phi_1$$

$$-\frac{B_0}{\Omega_d}\left(\frac{\partial^2}{\partial t^2} + \Omega_d^2\right)\frac{\partial^2 \varphi_1}{\partial z^2} + \left[\Omega_d \vec{e}_z \times \nabla_\perp \frac{\partial \phi_1}{\partial t} + \nabla_\perp \frac{\partial^2 \phi_1}{\partial t^2}\right.$$

$$\left. - B_0 \vec{e}_z \times \nabla_\perp \frac{\partial \varphi_1}{\partial t} - \frac{B_0}{\Omega_d} \nabla_\perp \frac{\partial^2 \varphi_1}{\partial t^2}\right] \nabla_\perp \ln n_{d0} = 0. \tag{2}$$

$$\nabla_\perp^2 \varphi_1 + \frac{\partial^2 \varphi_1}{\partial z^2} = -\omega_j^2 \frac{e\phi_1}{\kappa T_{ef}}, \quad \omega_j^2 = 4\pi G m_d n_{d0}, \quad \Omega_d = eZ_d B_0/m_d, \tag{3}$$

$$c_d^2 = \kappa T_{ef} Z_d/m_d \equiv \omega_{pd}^2 \lambda_d^2, \quad 1/\lambda_d^2 = 1/\lambda_i^2 + 1/\lambda_e^2 \equiv \omega_{pe}^2/v_{Te}^2 + \omega_{pi}^2/v_{Ti}^2,$$

$$\omega_{pd}^2 = e^2 Z_d^2 n_{d0}/\varepsilon_0 m_d, \quad \omega_{pe,i}^2 = e^2 n_{e0,i0}/\varepsilon_0 m_{e,i}, \quad T_{ef} = \frac{Z_d n_{d0} T_i T_e}{n_{i0} T_e + n_{e0} T_i}.$$

- Short wave-lengths (or for a laboratory plasma) $\Rightarrow$ the self-gravity effects can be ignored $\Rightarrow$ coupled dust-acoustic (DA), dust-cyclotron (DC), and dust-drift (DD) waves.
- This is most clearly seen in the Cartesian geometry (for an unbounded plasma) when for parallel propagation one obtains a DA mode $\omega^2 = c_d^2 k_z^2$; for the nearly perpendicular case without the density gradient one finds a DC wave $\omega^2 = \Omega_d^2 + c_d^2 k_\perp^2$; finally in the presence of the perpendicular density gradient and for low frequency limit $(\omega \ll \Omega_d)$ we have a DD wave described by $\omega^2 = c_d^2 \vec{k}_\perp \nabla_\perp (\ln n_{d0})/[\Omega_d(1 + k_\perp^2 \rho_d^2)]$, where $\rho_d = c_d/\Omega_d$.

# Analytical eigenfunctions

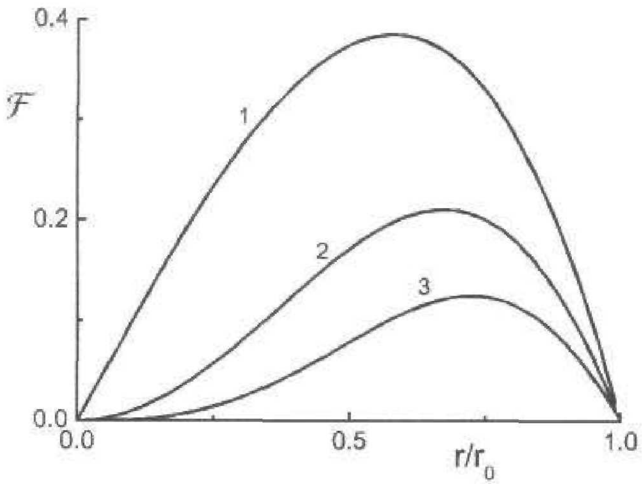


*No gravity; Kummer confluent hypergeometric functions;* $m = 1, 2, 3$.

Phys. Plasmas, Vol. 11, No. 5, May 2004

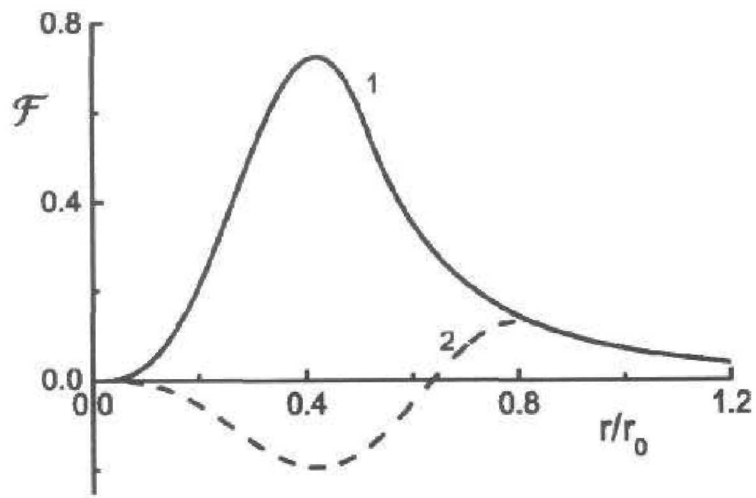


*Self-gravitating plasma; Bessel functions*

# Outline

- Eigen-mode equation (Vranjes and Poedts PoP **12**, 064501 (2005):

$$\left[\frac{\partial^2}{\partial r^2}+\left(\frac{1}{r}-\frac{k_z v_{i0}'(r)}{\omega-k_z v_{i0}(r)}\right)\frac{\partial}{\partial r}-\frac{m^2}{r^2}+\frac{k_z^2}{(\omega-k_z v_{i0}(r))^2}\right.$$
$$\left.-\frac{1}{\rho_s^2}-\frac{m}{r}\frac{1}{\omega-k_z v_{i0}(r)}\left(\frac{n_0'(r)}{n_0(r)}+\frac{k_z v_{i0}'(r)}{\omega-k_z v_{i0}(r)}\right)\right]\Phi_1(r)=0.$$

$$v_0(r)=a_1+a_2\exp(-ar^2/2),$$
$$n_0(r)=N_0\exp\left\{\frac{1}{2m}\left[\exp\left(-\frac{ar^2}{2}\right)\left[-\frac{2a_2bk_z}{a}-\frac{2a_2k_z}{a\rho_s^2}-\frac{2k_z\exp(ar^2)}{aa_2}\right.\right.\right.$$
$$\left.\left.\left.-amr^2\exp\left(\frac{ar^2}{2}\right)+2a_2k_zc\exp\left(\frac{ar^2}{2}\right)\right]\right]\right\}$$

# Streaming plasma: equilibrium quantities

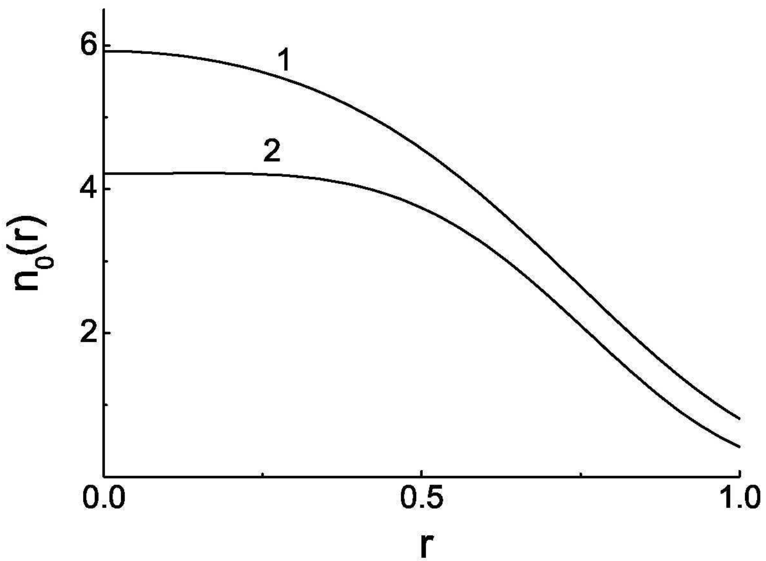


*Density profile in radial direction*

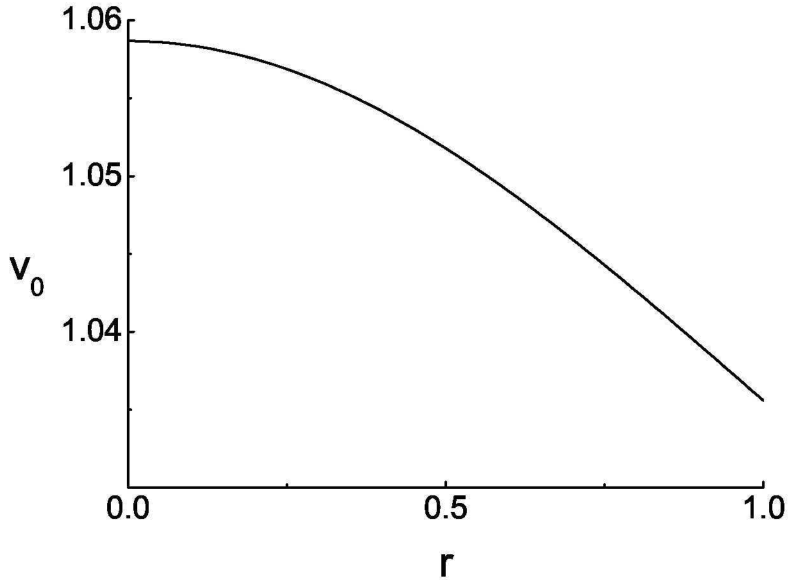


*Radial profile of the axial velocity.*

# Streaming plasma: eigenmode

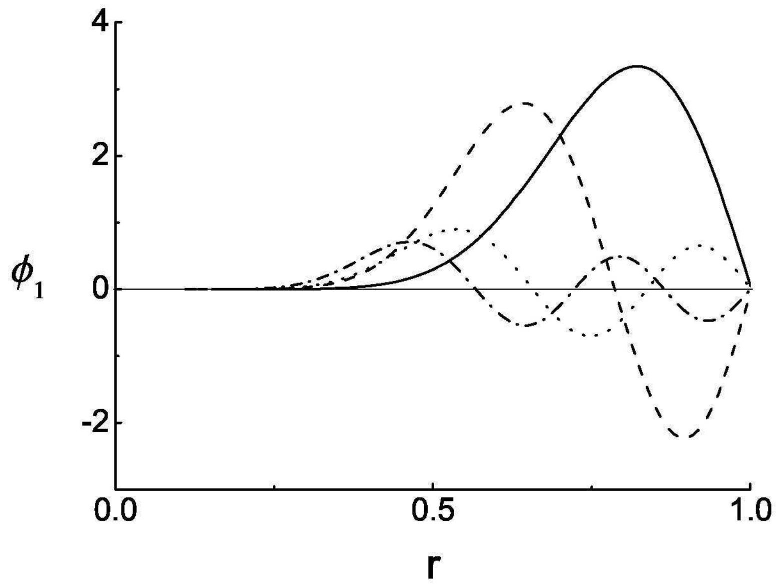


*Radial eigen-modes. J. Vranjes and S. Poedts, Phys. Plasmas* **12**, *064501 (2005).*

# Streaming plasma: contour plot

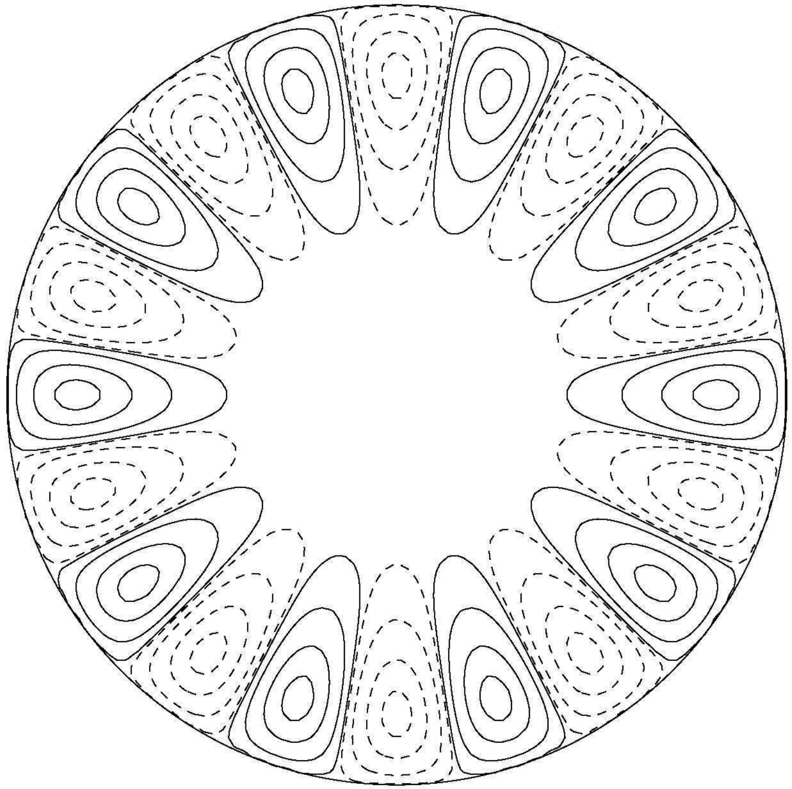

*The cross section of the potential for $m = 10$ and the first radial eigen-mode. Dashed lines denote negative part of the wave potential.*

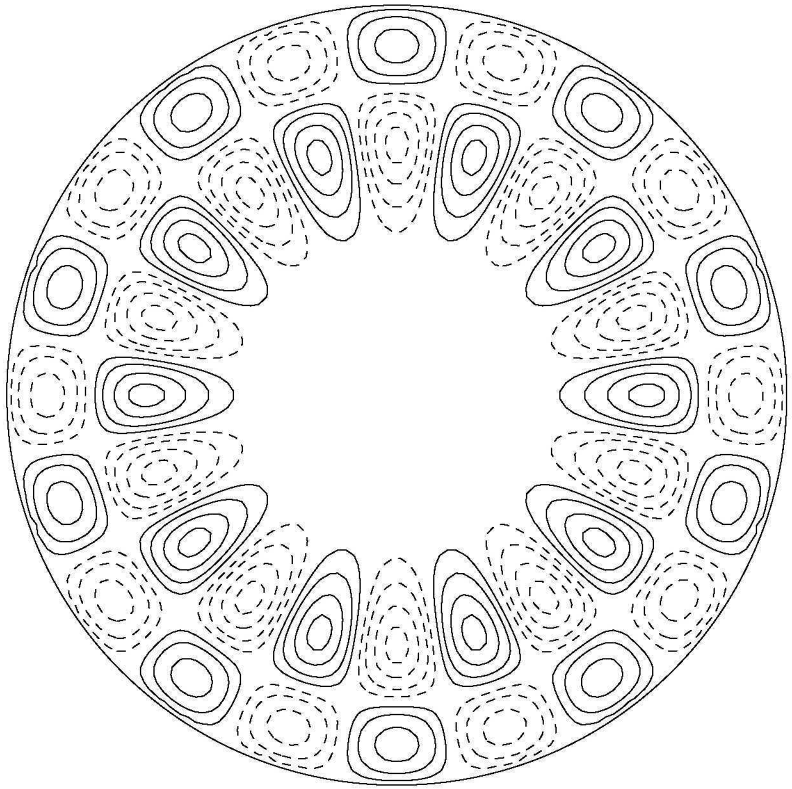

*The case of the second radial eigen-mode.*

# Experimental example

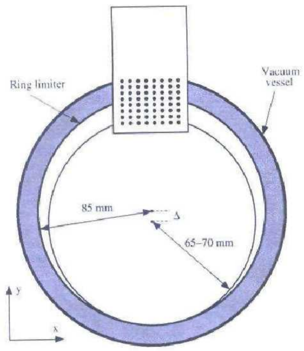


**Figure 1.** Scheme of the experimental setup. The picture shows a scheme of the poloidal section of the CASTOR tokamak where the array of probes has been inserted. The plasma, shifted downwards, is also depicted.

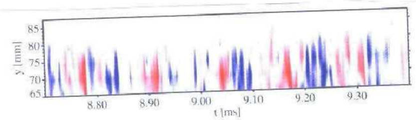


**Figure 2.** Floating potential measured by one column of probes plotted as a function of time and radial position. Blue indicates negative values and red indicates positive values. The peak values are ±27 V.

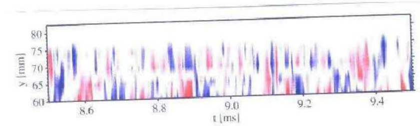


**Figure 6.** Floating potential measured by one column of probes plotted as a function of time and radial position (as in figure 2). Blue indicates negative values and red indicates positive values. The peak values are ±31.4 V. The presence of the LCFS at $y \approx 68$ cm is seen as a white line separating structures of opposite polarity.

*E. Martines et al. Plasma Phys. Control. Fusion* **44**, *351 (2002)*

# Outline

# Model

- Details in: Vranjes and Poedts, PoP **14**, 112106 (2007).
- Plasma in the magnetic field $\vec{B}_0 = B_0\vec{e}_z$; equilibrium density gradient in the direction both perpendicular and parallel to the magnetic lines.
- Density perturbations, electrostatic wave, oblique propagation:

$$\frac{1}{n_0}\frac{\partial^2 n_1}{\partial t^2} + \nabla_\perp \cdot \frac{\partial \vec{v}_{i\perp 1}}{\partial t} + \frac{\partial}{\partial z}\frac{\partial v_{iz1}}{\partial t} + \frac{\partial \vec{v}_{i\perp 1}}{\partial t} \cdot \frac{\nabla_\perp n_0}{n_0} + \frac{\partial v_{iz1}}{\partial t}\frac{1}{n_0}\frac{\partial n_0}{\partial z} = 0, \quad (4)$$

$$\frac{\partial \vec{v}_{i\perp 1}}{\partial t} = \frac{1}{B_0}\vec{e}_z \times \nabla_\perp \frac{\partial \phi_1}{\partial t} - \frac{1}{\Omega_i B_0}\frac{\partial^2}{\partial t^2}\nabla_\perp \phi_1, \quad (5)$$

$$\frac{\partial v_{iz1}}{\partial t} = -\frac{e}{m_i}\frac{\partial \phi_1}{\partial z}. \quad (6)$$

# Cartesian geometry

- Perturbations of the form $\hat{f}(x,z)\exp(-i\omega t + ik_y y)$ and a plasma with $\nabla n_0 = \vec{e}_x \partial n_0/\partial x + \vec{e}_z \partial n_0/\partial z$.

$$\left(\frac{\partial^2}{\partial z^2} - \frac{\omega^2}{\Omega_i^2}\frac{\partial^2}{\partial x^2}\right)\Phi + \frac{1}{n_0}\frac{\partial n_0}{\partial z}\frac{\partial \Phi}{\partial z} + \frac{\omega k_y}{\Omega_i}\frac{1}{n_0}\frac{\partial n_0}{\partial x}\Phi + \frac{\omega^2}{c_s^2}\left(1 + k_y^2\rho_s^2\right)\Phi = 0, \tag{7}$$

$$\Phi(x,z) = \frac{e\hat{\phi}_1(x,z)}{\kappa T_e} = \frac{\hat{n}_1}{n_0}, \quad c_s^2 = \frac{\kappa T_e}{m_i}, \quad \rho_s = \frac{c_s}{\Omega_i}.$$

- Eq. (7): the normalized amplitude of the coupled ion acoustic wave $\omega^2 = k_z^2 c_s^2$, and the drift wave

$$\omega = \omega_{*e}/(1 + k_y^2\rho_s^2), \quad \omega_{*e} = -k_y c_s^2 h_x/\Omega_i, \quad h_\alpha = \frac{1}{n_0}\frac{\partial n_0}{\partial \alpha}, \quad \alpha = x, z.$$

## Some limits

A.

- Introduce $h_\alpha^{-1} \sim L_\alpha$, $\alpha = x, z$; $\partial^2/\partial x^2$ can be omitted provided that $L_x/L_z > \omega/\Omega_i$. For exponential density in the perpendicular direction $h_x$ constant, and from (7), assuming the wave

$$\Phi(x,z) \simeq \hat{f}(z)\cos k_z z,$$

$$\Rightarrow \quad \hat{f}''(z) + h_z \hat{f}'(z) + \left[\frac{\omega^2}{c_s^2}\left(1 + k_y^2\rho_s^2\right) + \frac{\omega k_y}{\Omega_i} h_x - k_z^2\right]\hat{f}(z) = 0, \tag{8}$$

$$2\hat{f}'(z) + h_z \hat{f}(z) = 0. \tag{9}$$

- Eqs. (8), (9) valid for any function $h_z$.
- From (9): $\hat{f}(z) = f_0/[n_0(z)]^{1/2}$, $f_0$ - integration constant.

- Eq. (8) yields the dispersion equation for the coupled drift and IA waves,

$$\omega^2\left(1+k_y^2\rho_s^2\right)-\omega_{*e}\omega-k_z^2c_s^2-\frac{c_s^2}{\sqrt{n_0(z)}}\frac{\partial^2[\sqrt{n_0(z)}]}{\partial z^2}=0. \tag{10}$$

- The wave potential:

$$\Phi(x,z)\approx\frac{f_0}{n_0(z)^{1/2}}\cos k_z z, \tag{11}$$

$$k_z=\left\{\frac{\omega^2}{c_s^2}\left(1+k_y^2\rho_s^2\right)+\frac{\omega k_y h_x}{\Omega_i}-\frac{1}{\sqrt{n_0(z)}}\frac{\partial^2[\sqrt{n_0(z)}]}{\partial z^2}\right\}^{1/2}=const.$$

- The drift-IA wave grows/decreases for a decreasing/increasing density along the magnetic lines. The exponential density in the perp. direction determines the drift part.

- Eq. (8) yields the dispersion equation for the coupled drift and IA waves,

$$\omega^2\left(1+k_y^2\rho_s^2\right)-\omega_{*e}\omega-k_z^2c_s^2-\frac{c_s^2}{\sqrt{n_0(z)}}\frac{\partial^2[\sqrt{n_0(z)}]}{\partial z^2}=0. \qquad (12)$$

- The wave potential:

$$\Phi(x,z)\approx\frac{f_0}{n_0(z)^{1/2}}\cos k_z z, \qquad (13)$$

$$k_z=\left\{\frac{\omega^2}{c_s^2}\left(1+k_y^2\rho_s^2\right)+\frac{\omega k_y h_x}{\Omega_i}-\frac{1}{\sqrt{n_0(z)}}\frac{\partial^2[\sqrt{n_0(z)}]}{\partial z^2}\right\}^{1/2}=const.$$

- The drift-IA wave grows/decreases for a decreasing/increasing density along the magnetic lines. The exponential density in the perp. direction determines the drift part.

- $\omega, k_y, k_z$ are constant if $\left[(n_0(z))^{1/2}\right]'' / (n_0(z))^{1/2}$ is constant.

  i) Exponential equilibrium profiles in both directions;
  $n_0(x, z) = N_0 \exp(\pm x/L_x + bz)$, $b > 0$, or $b < 0$. The dispersion equation for the modified drift-IA wave:

$$\omega^2 \left(1 + k_y^2 \rho_s^2\right) - \omega_{*e}\omega - c_s^2 (k_z^2 + b^2/4) = 0. \qquad (14)$$

  $\Rightarrow$ The cut-off *frequency* for the IA mode propagating along the exponentially varying density.
  i) In the case $n_0(x, z) = N_0 \exp(\pm x/L_x) \cos^2 bz$, or
  $n_0(x, z) = N_0 \exp(\pm x/L_x) \sin^2 bz$ (the local variation in the $z$-direction is monotonous, i.e., non-oscillatory, implying that $|bz| \ll \pi/2$):

$$\omega^2 \left(1 + k_y^2 \rho_s^2\right) - \omega_{*e}\omega - c_s^2 (k_z^2 - b^2) = 0. \qquad (15)$$

  $\Rightarrow$ the cut-off *wave number* $k_z$.

# Experiment: Doucet et al. PF **17**, 1738 (1974)

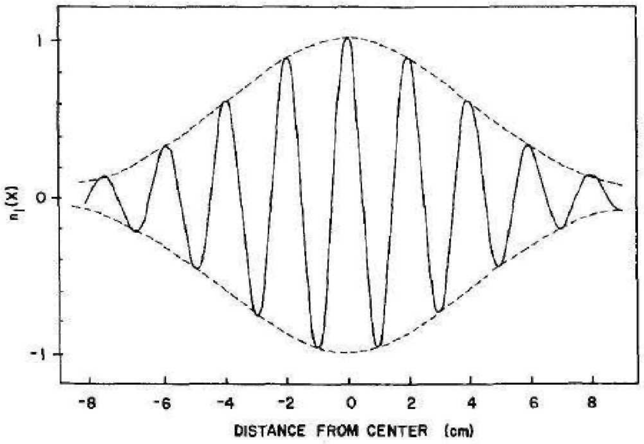


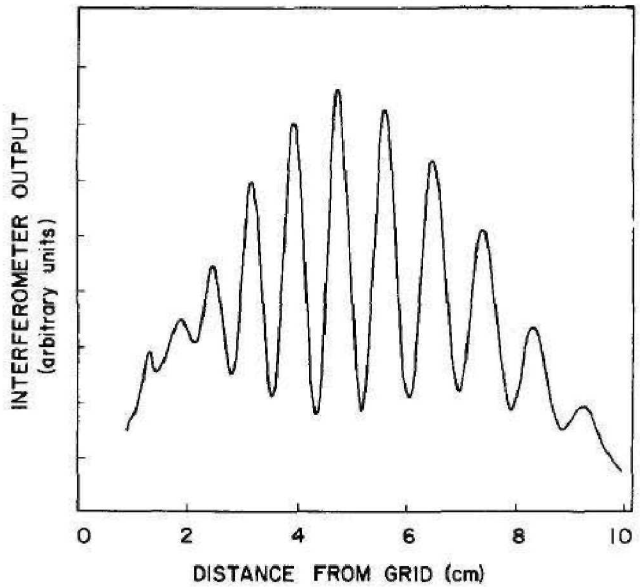

B.

- Small $\partial^2/\partial x^2$ part in Eq. (7) and $n_0(x,z) = N_0 \exp(\pm x/L_x - \kappa_z^2 z^2)$

$$\Phi''(z) - 2\kappa_z^2 z\Phi'(z) + a_0\Phi(z) = 0, \quad a_0 = \frac{\omega^2}{c_s^2}\left(1 + k_y^2\rho_s^2\right) + \frac{\omega k_y h_x}{\Omega_i}. \tag{16}$$

- The general solution in terms of the Kummer confluent hypergeometric functions

$$\Phi(z) = C_1 \cdot {}_1F_1\left[-\frac{a_0}{4\kappa_z^2}, \frac{1}{2}, \kappa_z^2 z^2\right] + C_2 \cdot z \cdot {}_1F_1\left[\frac{1}{2} - \frac{a_0}{4\kappa_z^2}, \frac{3}{2}, \kappa_z^2 z^2\right]. \tag{17}$$

- Depending on the values of $\alpha, \beta$, ${}_1F_1[\alpha, \beta, \chi]$ includes various special functions, like the Hermite functions, the Error Integral, the Parabolic Cylinder functions, etc. Symmetric density profile along the magnetic lines $\Rightarrow$ keep the even solutions in (17).

- According to well known features of the functions ${}_1F_1[\alpha, \beta, \chi]$, for large negative $\alpha$, bounded $\beta$ and real $\chi$, the solution is oscillatory and growing in the $\chi$-direction, and can be written as

$$
{}_1F_1 \approx \Gamma(\beta)\pi^{-1/2}\exp(\chi/2)(\beta\chi/2 - \alpha\chi)^{1/2-\beta/2}\cos\Big[(2\beta\chi - 4\alpha\chi)^{1/2} - \beta\pi/2 + \pi/4\Big].
$$

- $\Gamma$ - the Gamma function. Hence, the amplitude of the wave potential (and the relative density perturbation $\hat{n}_1/n_0$) grows in the direction of the decreasing density $n_0$.

C.

- The complete Eq. (7) can be solved by the separation of variables

$$
\Phi(x, z) = \psi(x) \cdot \xi(z).
$$

$\Rightarrow$

$$\psi\frac{d^2\xi}{dz^2} - a_1\xi\frac{d^2\psi}{dx^2} + h_z\psi\frac{d\xi}{dz} + (a_2h_x + a_3)\psi\xi = 0, \tag{18}$$

$$a_1 = \frac{\omega^2}{\Omega_i^2}, \quad a_2 = \frac{\omega k_y}{\Omega_i}, \quad a_3 = \frac{\omega^2}{c_s^2}\left(1 + k_y^2\rho_s^2\right).$$

This yields

$$\frac{d^2\psi(x)}{dx^2} - \frac{a_2h_x + \alpha}{a_1}\psi(x) = 0, \tag{19}$$

$$\frac{d^2\xi(z)}{dz^2} + h_z\frac{d\xi(z)}{dz} + (a_3 - \alpha)\xi(z) = 0. \tag{20}$$

$\alpha$ - arbitrary constant which appears due to the separation of variables. The equations can be solved analytically for a number of functions $h_x, h_z$.

- Gaussian equilibrium density in the $z$-direction $n_0 \sim \exp(-\kappa_z^2 z^2)$, the solution of Eq. (20) is the same as (17) where only we have $a_3 - \alpha$ instead of $a_0$.

  i) If we also have $n_0 \sim \exp(\kappa_x^2 x^2)$ locally, then $h_x = 2\kappa_x^2 x$ and the solution of Eq. (19) is

$$\psi(x) = D_1 \cdot B_i \left[ d_1^{1/3} \left( x + \frac{d_2}{d_1} \right) \right] + D_2 \cdot A_i \left[ d_1^{1/3} \left( x + \frac{d_2}{d_1} \right) \right]. \quad (21)$$

  Here, $d_1 = 2\kappa_x^2 a_2/a_1$, $d_2 = \alpha/a_1$, and $A_i, B_i$ are the Airy functions.
  ii) For a locally exponential density in the $x$-direction, $n_0 \sim \exp(\kappa_x x)$, where $\kappa_x > 0$ or $\kappa_x < 0$, Eq. (19) becomes of the form $\psi''(x) \pm |c_0|\psi(x) = 0$, $c_0 = (a_2\kappa_x + \alpha)/a_1$. The solutions (for the sign $+$) are $\psi = D_1 \cdot \sin(xc_0^{1/2}) + D_2 \cdot \cos(xc_0^{1/2})$, otherwise $\psi = D_1 \cdot \exp(-xc_0^{1/2}) + D_2 \cdot \exp(xc_0^{1/2})$.

# Cylindric plasma - global modes

- Cylindric plasma which extends up to $r = r_0$; density $n_0 = n_0(r, z)$; perturbations $f(r, z)\exp(-i\omega t + im\theta)$;

$$\left[\frac{\partial^2}{\partial r^2} + \left(\frac{1}{r} + h_r\right)\frac{\partial}{\partial r} - \frac{m^2}{r^2} - \frac{r_0^2}{\rho_s^2} - \frac{\Omega_i}{\omega}\frac{m}{r}h_r - \frac{\Omega_i^2}{\omega^2}\left(\frac{\partial^2}{\partial z^2} + h_z\frac{\partial}{\partial z}\right)\right]\Phi(r, z) = 0. \tag{22}$$

All spatial variables in units of $r_0$, and $h_r = (\partial n_0/\partial r)/n_0$.

- A good representative of various plasmas: Gaussian equilibrium density in both directions $n_0(r, z) = N_0\exp(-\kappa_r^2 r^2 - \kappa_z^2 z^2)$, where $\kappa_r \neq \kappa_z$ and typically $\kappa_r/\kappa_z \gg 1$, hence $h_r = -2\kappa_r^2 r$, $h_z = -2\kappa_z^2 z$.

- Introducing as earlier $\Phi(r,z) = \psi(r)\xi(z)$, from (22):

$$\left[\frac{\partial^2}{\partial r^2} + \left(\frac{1}{r} - 2\kappa_r^2 r\right)\frac{\partial}{\partial r} - \frac{m^2}{r^2} + b_0\right]\psi(r) = 0, \tag{23}$$

$$\left(\frac{\partial^2}{\partial z^2} - 2\kappa_z^2 z\frac{\partial}{\partial z} + a_0\right)\xi(z) = 0. \tag{24}$$

$$b_0 = \frac{2m\kappa_r^2\Omega_i}{\omega} - \alpha, \quad a_0 = \frac{r_0^2\omega^2}{c_s^2} - \frac{\alpha\omega^2}{\Omega_i^2}. \tag{25}$$

- $\alpha$ - arbitrary constant due to the separation of variables. The drift and IA modes are decoupled for $\alpha = 0$. In the homogeneous case (24) yields the IA wave $\omega^2 = k_z^2 c_s^2$, otherwise it gives the axially dependent mode amplitude.

- The general solutions of Eqs. (23), (24) are, respectively,

$$\psi(r) = C_1 \cdot r^{-m} \cdot {}_1F_1\left[-\frac{b_0}{4\kappa_r^2} - \frac{m}{2}, 1-m, \kappa_r^2 r^2\right]$$

$$+C_2 \cdot r^m \cdot {}_1F_1\left[-\frac{b_0}{4\kappa_r^2} + \frac{m}{2}, 1+m, \kappa_r^2 r^2\right], \tag{26}$$

$$\xi(z) = D_1 \cdot {}_1F_1\left[-\frac{a_0}{4\kappa_z^2}, \frac{1}{2}, \kappa_z^2 z^2\right] + D_2 \cdot z \cdot {}_1F_1\left[\frac{1}{2} - \frac{a_0}{4\kappa_z^2 \Omega_i^2}, \frac{3}{2}, \kappa_z^2 z^2\right]. \tag{27}$$

- Well behaved solutions [non-singular in $(r, z)$-plain and even in $\pm z$ directions] imply $C_1 = D_2 = 0$. In laboratory conditions the potential vanishes at least at $r = 0$, and $r = r_0$, resembling a radially standing drift wave. Due to limited axial length in laboratory situations a standing wave may appear in the axial direction too.

- Electron-reach operations: the lowest eigenmode will satisfy $k_z L \simeq \pi$, or $\lambda_z \simeq 2L$. Here $L$ is the distance between the two sheaths formed at both ends.
- Ion-reach operations: the standing wave may appear with the maximum in the middle, but with a finite potential at the ends/sheaths, corresponding to the axial wavelength larger than $2L$. Details in F. F Chen, Phys. Fluids **22**, 2346 (1979); experimental observation in Rowberg and Wong, Phys. Fluids **13**, 661 (1970).
- In space plasmas, like in the highly elongated magnetic flux tubes in the solar atmosphere, in the axial direction we may simply have a propagating IA wave.

- From Eqs. (25) eliminate $\alpha$:

$$\omega^2\left(1+b_0\frac{\rho_s^2}{r_0^2}\right)-\frac{2mc_s^2\kappa_r^2}{\Omega_i r_0^2}\,\omega-\frac{a_0c_s^2}{r_0^2}=0. \tag{28}$$

- In physical units $\omega^2(1+b_0\rho_s^2)-2m\Omega_i\kappa_r^2\rho_s^2\omega-a_0c_s^2=0$.
- The parameter $b_0$ is to be determined from the requirement of vanishing solutions at $r_0$. Because Eq. (26) may contain oscillatory solutions (in $r$), this implies a sequence of discrete values for $b_0$.
- $a_0$: a free parameter for an infinite plasma column, otherwise to be determined from the requirement $\xi(L/2)=0$ for (oscillatory) solutions in the limited axial direction, $\pm L/2$ determines the two ends of the plasma column. In the later case, we have only a drift wave propagating in the poloidal direction, determined by the poloidal number $m$, and having a standing wave structure in both radial and axial directions.

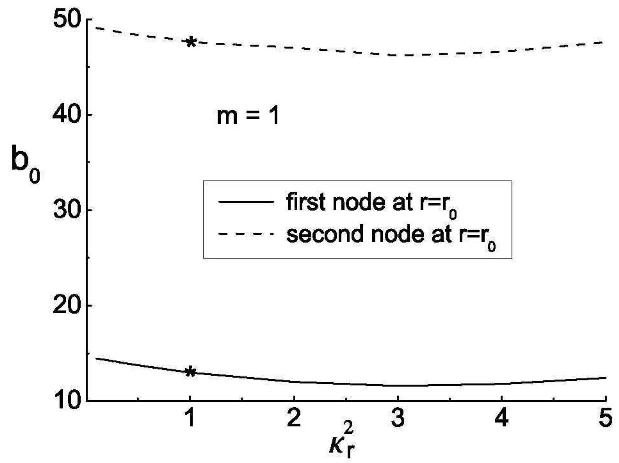


*Eigenvalues [for the poloidal drift wave number $m = 1$] for different radial density profiles, yielding a standing wave solution in the radial direction.*

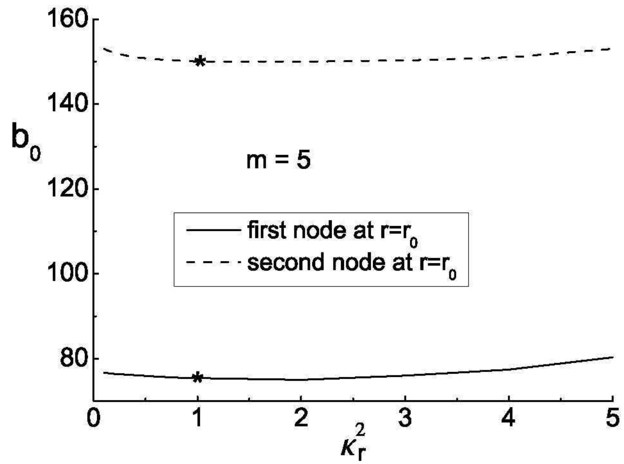


*Similar, but for $m = 5$.*

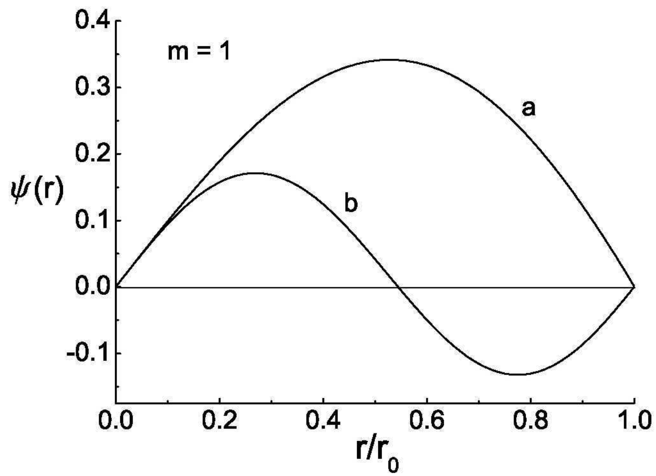


*The eigenfunctions Eqs. (26) (in arbitrary units) for $m = 1$, and for $\kappa_r^2 = 1$, $b_0 = 13$ (line a - the first eigenfunction), and $b_0 = 47.6$ (line b - the second eigenfunction). These parameters are denoted by $*$ in previous figures*

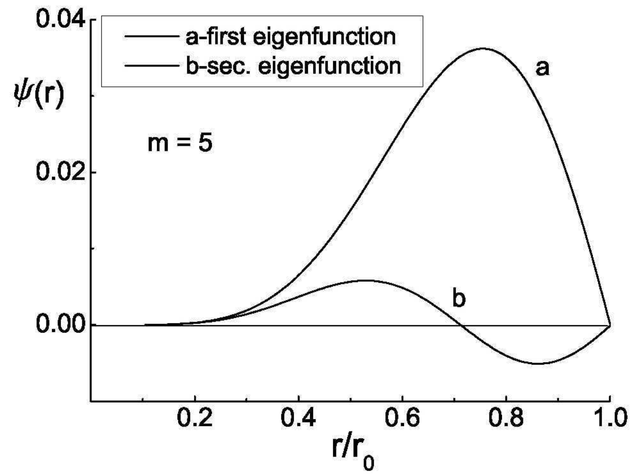


*The eigen-functions (in arbitrary units) for $m = 5$ and $b_0 = 84, 156$, and $\kappa_r^2 = 6$.*

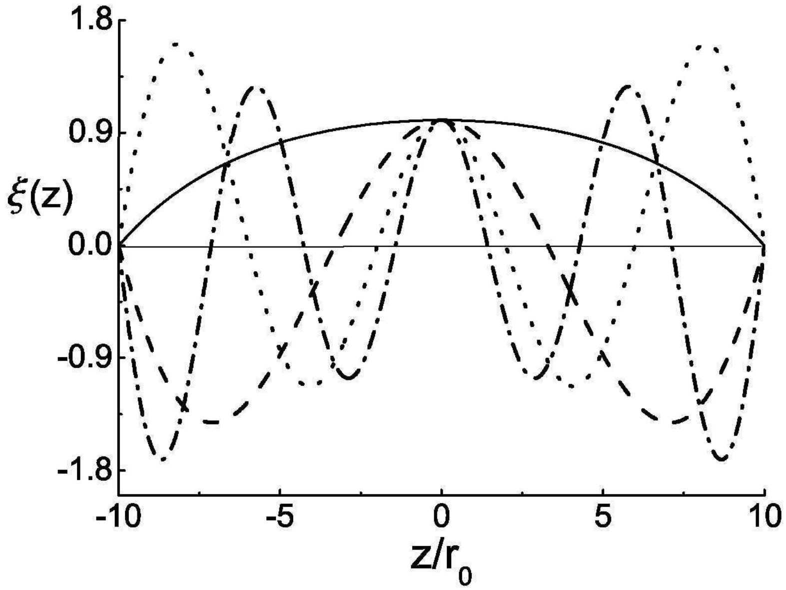


*The first four* *axial* *eigenfunctions. Here* $\kappa_z^2 = 0.014 \Rightarrow n_0(z = L)/N_0 = 0.24$. *Axial eigenvalues are* $a_0 = 0.013,\ 0.214,\ 0.609,\ 1.202$.

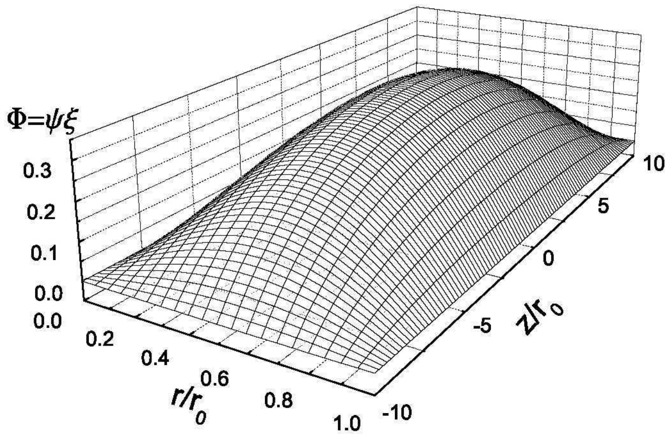


*The standing wave potential in the $r, z$-plain for the drift mode $m = 1$ and lowest eigenfunctions in both r- and z-directions; $\kappa_r = 1$, $b_0 = 13.3$, $\kappa_z^2 = 0.014$, $a_0 = 0.013$.*

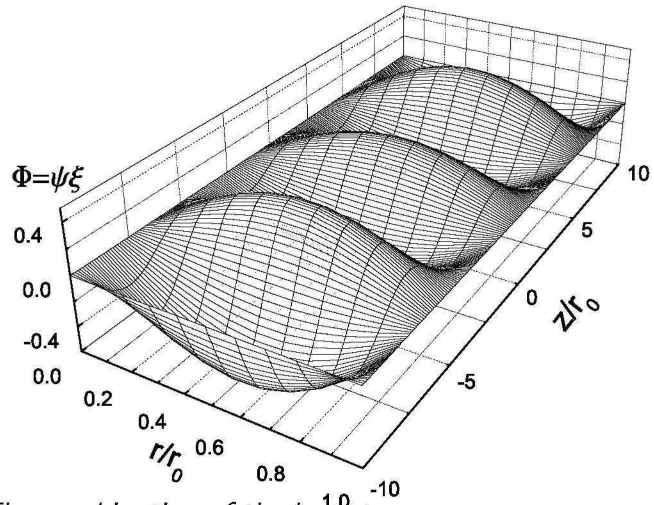


*The combination of the lowest eigenfunction in the r-direction with the 4th eigenfunction in the z-direction; $\kappa_r = 1$, $b_0 = 13.3$, $\kappa_z^2 = 0.014$, $a_0 = 1.2015$, and $m = 1$.*

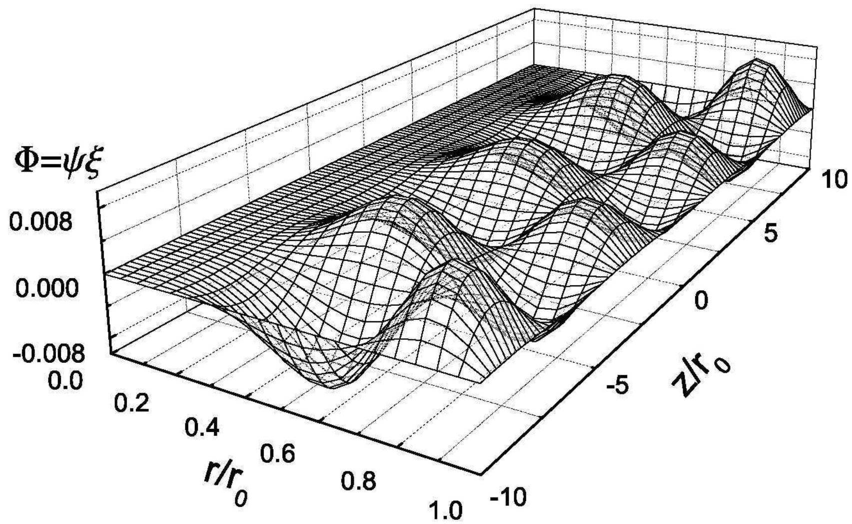


*$m = 5$, and the combination of the second eigenfunction in r-direction with the 4th eigenfunction in z-direction; $\kappa_r = 1$, $b_0 = 150$, $\kappa_z^2 = 0.014$, $a_0 = 1.2015$.*

# Outline

- Global modes $\Leftrightarrow$ global plasma properties.
- The behavior of coupled drift and ion acoustic modes is discussed in plasmas with density gradients perpendicular as well as parallel to the magnetic field lines.
- The density gradient in the direction of propagation of an IA wave is known to cause the growth of the IA wave potential amplitude and the relative density perturbation.
- The presence of both of these gradients in a nonlocal analysis implies solving a double eigenvalue problem.
- In the past, problems of that kind have been treated numerically, and separately for the axial and perpendicular directions.

- The wave analysis performed both in Cartesian and cylindric geometry; eigenvalue equations solved *analytically* for a number of radial and axial density profiles.
- General solutions found; radially and axially varying wave amplitudes.

- Improvement of the model possible:
  i. (electron) collisions $\Rightarrow$ instability,
  ii. hot ion effects,
  iii. electromagnetic effects (coupling with kinetic Alfvén waves).
- All these effects studied in different context in: Vranjes and Poedts, Growing drift-Alfvén modes in collisional solar plasma, Astron. Astrophys. **458**, 635 (2006).
  iv. nonlinear electromagnetic equations: Vranjes and Poedts, Drift-Alfven eigenmodes in inhomogeneous plasma, Phys. Plasmas **13**, 032107 (2006).

- The momentum equations for ions and electrons

$$m_i n_i \left[\frac{\partial \vec{v}_i}{\partial t} + (\vec{v}_i \cdot \nabla)\vec{v}_i\right] = e n_i \left(-\nabla\phi - \frac{\partial A_z}{\partial t}\vec{e}_z + \vec{v}_i \times \vec{B}\right)$$

$$-\kappa T_i \nabla n_i - \nabla \cdot \Pi_i - m_i n_i \nu_i \vec{v}_i, \tag{29}$$

$$m_e n_e \left[\frac{\partial \vec{v}_e}{\partial t} + (\vec{v}_e \cdot \nabla)\vec{v}_e\right] = -e n_i \left(-\nabla\phi - \frac{\partial A_z}{\partial t}\vec{e}_z + \vec{v}_e \times \vec{B}\right)$$

$$-\kappa T_e \nabla n_e - \nabla \cdot \Pi_e - m_e n_e (\nu_e \vec{v}_e - \nu_{ei} \vec{v}_i). \tag{30}$$

- The procedure straightforward except for the term with the convective derivative in the polarization drift $\vec{v}_p$, i.e., $(\vec{v}_{i\perp}\cdot\nabla_\perp)\vec{e}_z\times\vec{v}_{i\perp}$, and the stress tensor contribution $\vec{v}_\pi$.
- For a small equilibrium density gradient, the last $\vec{v}_{i\perp}$ in $\vec{v}_p$ comprises only the leading order perturbed $\vec{E}\times\vec{B}$ and diamagnetic drifts ($\vec{v}_{E1}$ and $\vec{v}_{*i1}$), while the first $\vec{v}_i$ is the equilibrium ion diamagnetic drift $\vec{v}_{i0}=\kappa T_i\vec{e}_z\times\nabla_\perp n_{i0}/(eB_0n_{i0})=-\vec{v}_{e0}T_i/T_e$.
- The stress tensor part yields

$$\begin{aligned}\nabla_\perp\cdot(n\vec{v}_\pi)&=-\rho_i^2\nabla_\perp n_{i0}\cdot\nabla_\perp^2\vec{v}_{i\perp}-n_{i0}\rho_i^2\nabla_\perp^2\nabla_\perp\cdot\vec{v}_{i\perp}\\&=-\rho_i^2\nabla_\perp n_{i0}\cdot\nabla_\perp^2\vec{v}_{i\perp}+\frac{\rho_i^2n_{i0}}{\Omega_i}\frac{\partial}{\partial t}\nabla_\perp^4\left(\frac{\phi_1}{B_0}+\frac{v_{Ti}^2}{\Omega_i}\frac{n_{i1}}{n_{i0}}\right).\end{aligned}\tag{31}$$

- The first term in this expression, within the second order approximation limit, cancels out with $(\vec{v}_{i0}\cdot\nabla_\perp)\vec{e}_z\times\vec{v}_{i\perp}$ from the convective derivative in the polarization drift which appears in $\nabla_\perp\cdot(n_i\vec{v}_p)$.

- The parallel electron momentum

$$\left(\frac{\partial}{\partial t} + \vec{v}_{e0}\nabla_\perp\right) A_{z1} + \frac{\partial \phi_1}{\partial z} - \frac{\kappa T_e}{n_{e0} e}\frac{\partial n_{e1}}{\partial z} - \frac{m_e \nu_e}{\mu_0 e^2 n_{e0}}\nabla_\perp^2 A_{z1} = 0. \quad (32)$$

- The electron continuity

$$\frac{\partial n_{e1}}{\partial t} + \frac{1}{B_0}(\vec{e}_z \times \nabla_\perp \phi_1)\cdot \nabla_\perp n_{e0} + \frac{1}{\mu_0 e}\frac{\partial}{\partial z}\nabla_\perp^2 A_{z1} = 0. \quad (33)$$

- The ion continuity

$$\frac{\partial}{\partial t}\left(\frac{n_{i1}}{n_{i0}}\right) + \frac{1}{B_0}\vec{e}_z \times \nabla_\perp \phi_1 \cdot \frac{\nabla_\perp n_{i0}}{n_{i0}} - \nu_i n_{i0}\rho_i^2 \nabla_\perp^2 \left(\frac{e\phi_1}{\kappa T_i} + \frac{n_{i1}}{n_{i0}}\right)$$

$$-n_{i0}\rho_i^2 \frac{\partial}{\partial t}\nabla_\perp^2 \left(\frac{e\phi_1}{\kappa T_i} + \frac{n_{i1}}{n_{i0}}\right) + \frac{\rho_i^2 n_{i0}}{\Omega_i}\frac{\partial}{\partial t}\nabla_\perp^4 \left(\frac{\phi_1}{B_0} + \frac{v_{Ti}^2}{\Omega_i}\frac{n_{i1}}{n_{i0}}\right) = 0. \quad (34)$$

- For global modes $|\rho_i \nabla_\perp| < 1$:

$$\left(\frac{\partial^2}{\partial r^2} + \frac{1}{r}\frac{\partial}{\partial r} - \frac{m^2}{r^2} + \eta^2\right)[\widehat{A}_{z1} + c\psi(r)] = 0. \tag{35}$$

$$\psi(r) = 0, \quad \text{or} \quad \psi(r) = c_1 \cosh[m\log(r)] + c_2 \sinh[m\log(r)]. \tag{36}$$

$$\eta^2 = \Big[\omega(\omega + i\nu_i)\left(\omega + ma\rho_s^2\Omega_i\right)\left(\omega - ma\rho_i^2\Omega_i\right)$$
$$-\omega k_z^2 c_a^2\left(\omega + ma\rho_s^2\Omega_i\right)\Big]\Big\{k_z^2 c_a^2(\omega + i\nu_i)\Big[\rho_s^2(1 - i\delta_1)\left(\omega - ma\rho_i^2\Omega_i\right)$$
$$+\rho_i^2(\omega + ma\rho_s^2\Omega_i)\Big]\Big\}^{-1}, \quad c = \frac{(\omega + ma\rho_s^2\Omega_i)}{k_z c_a^2 \rho_s^2 \eta^2 (1 - i\delta_1)}.$$

- Dispersion equation:

$$\eta^2 = \frac{\varepsilon_l^2}{r_0^2}. \tag{37}$$

$$\Rightarrow \quad \widehat{\phi}_1 = \frac{k_z^2 c_a^2}{(\omega + i\nu_i)(\omega - ma\rho_i^2\Omega_i)}\left[\omega - \rho_i^2(\omega + i\nu_i)\nabla_\perp^2\right]\widehat{A}_{z1} + \psi(r), \quad (38)$$

$$\Rightarrow \quad \widehat{n}_1 = \frac{k_z}{\mu_0 e\omega}\nabla_\perp^2 \widehat{A}_{z1} - \frac{m}{r}\frac{n_0'}{\omega B_0}\widehat{\phi}_1. \quad (39)$$


Thank you!